

Supporting Information for

**High Alkaline Ions Storage Capacities of Hollow Interwoven Structured
Sb/TiO₂ Particles: Galvanic Replacement Formation Mechanism and
Volumetric Buffer Effect**

Lin Zhou^{ab}, Yong Cheng^{a}, Qujiang Sun^{ac}, Lianshan Sun^a, Chunli Wang^{ab}, Xuxu Wang^{ab},
Dongming Yin^a, Limin Wang^a, Jun Ming^{a*}*

^a State Key Laboratory of Rare Earth Resource Utilization, Changchun Institute of Applied Chemistry, CAS, Changchun, 130022, China

^b University of Science and Technology of China, Hefei, P. R. China

^c University of Chinese Academy of Sciences, Beijing, 100049, China

*To whom correspondence should be addressed: cyong@ciac.ac.cn; jun.ming@ciac.ac.cn.

Methods and Characterizations

Synthesis of Hollow Interwoven Structured Sb/TiO₂. The template of nanosized Ti (30~300 nm) was purchased from Aladdin Reagent Co.; Ltd. (China) and stored in glove box. Typically, 2.281 g SbCl₃ were dispersed in 80 mL ethylene glycol first, in which 48 mg Ti powders were added under magnetic stirring in glove box. After the reaction for 15 min, the solution was then transferred to a Teflon-lined autoclave and maintained at 160 °C for 12 h. The autoclave was cooled down to room temperature naturally. The product of intermediates (*i.e.*; Sb/TiX) was filtrated and washed by absolute ethanol for several times and then dried under vacuum at 50 °C overnight. Calcination of the intermediates at 450 °C for 2 h under the flow Ar atmosphere give rise to hollow interwoven structured Sb/TiO₂. Besides, the solid composite of Sb/TiO₂ with the mass ratio of 4:1 were mixed by the TiO₂ and Sb particles for the comparative experiment. In this experiment, excess SbCl₃ was used to react with the Ti template, where the residual chloride ion (Cl⁻) in intermediate compounds (*i.e.*, Sb/TiX) was washed completely after the reaction. Besides, the Sb nanocrystals were protected under the inert Ar flow during the calcination.

Materials Characterizations. The morphology of products was characterized by the scanning electron microscopy (SEM) operating on a Hitachi S-4800 SEM analyzer, while the structural evolution and elemental mapping was observed by the transmission electron microscopy (TEM) on a FEI G2 S-Twin instrument. The crystallographic structure of samples were characterized by power X-ray diffractometer (XRD, Bruker D8 Focus) at a scan speed of 2° min⁻¹ with copper K α radiation. Note that the Ti template is very easily to be oxidized in XRD test, thus a mixed phase of Ti and TiO can be detected and abbreviated as Ti(O) in XRD description. The chemical component and valence status were collected using X-ray photoelectron spectrometer (XPS, ESCALABMKLL) with Al K α radiation, that emits 1.4866 keV x-ray with corresponding wavelength of 8.53 Å.

Electrochemical Measurements. The Sb/TiO₂ based electrode consist of the active material of Sb/TiO₂ composite, acetylene black, and carboxymethyl cellulose (CMC, Alfa Aesar) with a weight ratio of 7:2:1. The mixture was milled in distilled water to form a uniform slurry, and then it was casted on copper foil and dried in vacuum at 60 °C for 24 h. The electrode was then punched into circular electrode pieces and the areal density of active material is about 1.0 mg cm⁻². The cell was assembled in glove box filled with argon gas, in which the moisture and oxygen content was strictly controlled below 0.1 ppm. The CR-2025 type coin cell with the configuration of the metallic lithium or sodium foil counter | *Celgard* 2400 membrane separator | as-prepared electrode, in which the electrolyte of 1.0 M LiPF₆ in ethylene carbonate/diethylene carbonate (1/1 in volume) with 2% fluoroethylene carbonate (FEC) additive or the electrolyte of 1.0 M NaClO₄ in propylene carbonate (PC) with 5% FEC were used for lithium and sodium battery separately. The cut-off voltages for lithium and sodium battery were controlled at 0.01-2.5 V and 0.01-2.0 V respectively, where the galvanostatic charge-discharge curves were recorded by the programmable battery testing system (LAND CT2001A). The cyclic voltammogram (CV) under the scan rate of 0.1 mV s⁻¹ were tested by the *Bio-Logic VMP3* electrochemical workstation.

Table S1 Standard electrode potential of materials which can be reduced in theory by the metallic Ti.

Electrode progress	E ^A /V
Ti ²⁺ + 2e ⁻ → Ti	-1.63
Ti ³⁺ + 3e ⁻ → Ti	-1.37
Sn ²⁺ + 2e ⁻ → Sn	-0.138
Zn ²⁺ + 2e ⁻ → Zn	-0.7618
Cr ³⁺ + 3e ⁻ → Cr	-0.744
Cd ²⁺ + 2e ⁻ → Cd	-0.43
Co ²⁺ + 2e ⁻ → Co	-0.28
Ni ²⁺ + 2e ⁻ → Ni	-0.257
Pb ²⁺ + 2e ⁻ → Pb	-0.126
Fe ³⁺ + 3e ⁻ → Fe	-0.037
Bi ³⁺ + 3e ⁻ → Bi	0.308
Cu ²⁺ + 2e ⁻ → Cu	0.342
Ag ¹⁺ + e ⁻ → Ag	0.799
Au ¹⁺ + e ⁻ → Au	1.692

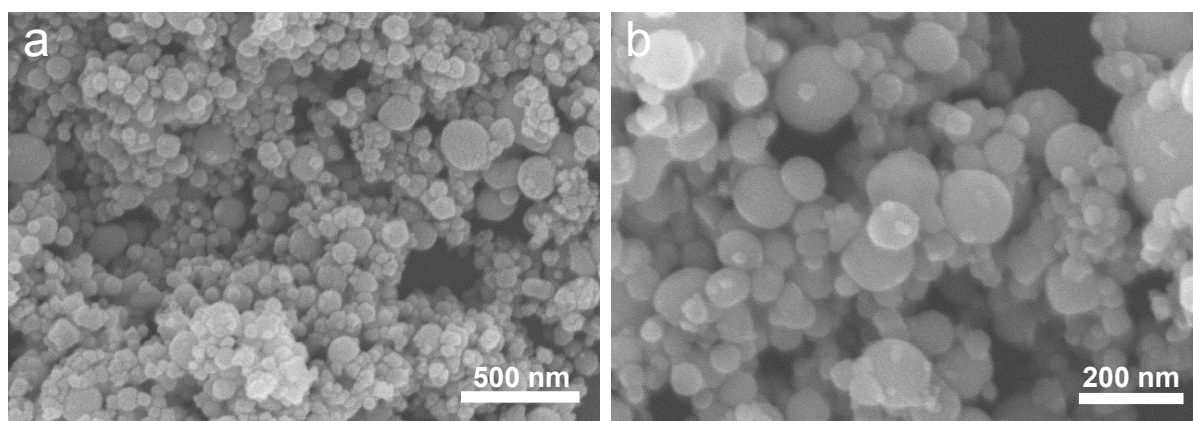


Figure S1 | SEM of Ti powders with (a) a low and (b) a high magnification. The results show that the Ti powders has a wide range of particle size distribution.

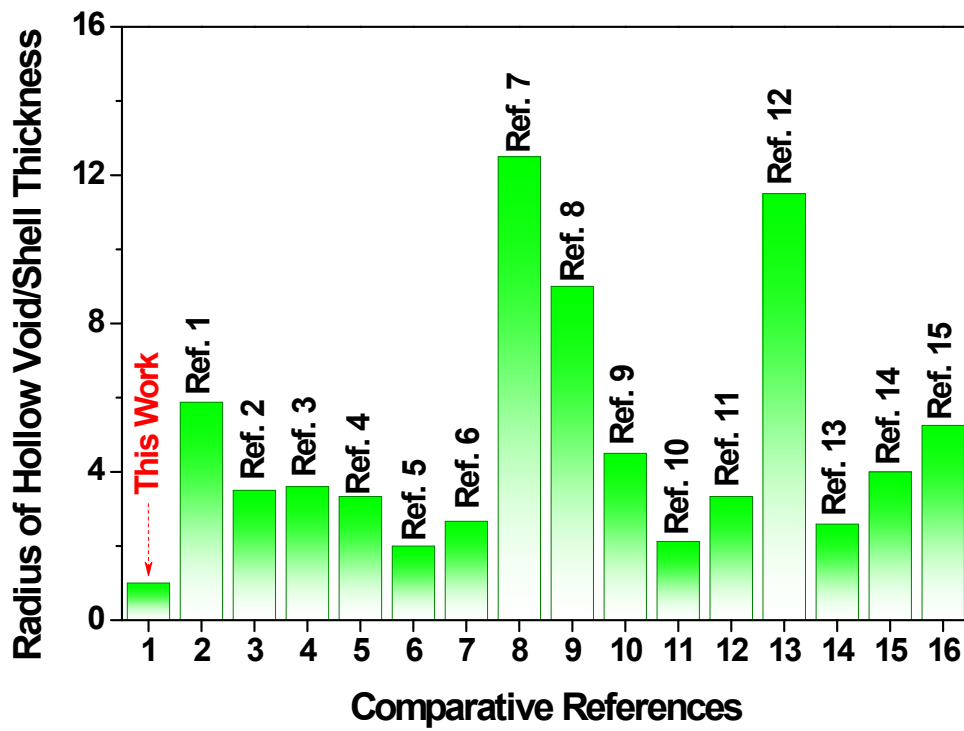


Figure S2 | Comparative ratio of the inner radius of hollow void and the shell thickness with the researches reported before.¹⁻¹⁵

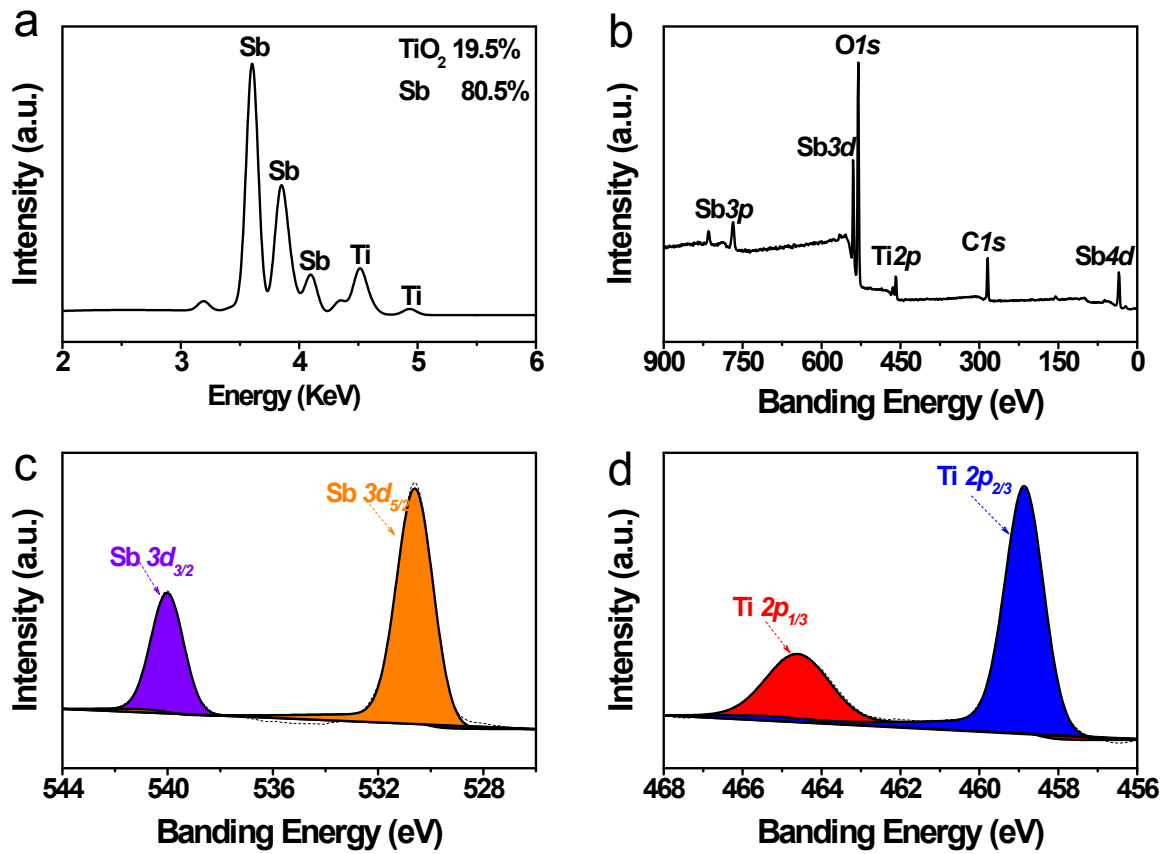


Figure S3 | Elemental and valence status analysis. (a) EDX and (b) XPS survey scan spectra, (c) Sb3d and (d) Ti2p of hollow interwoven structured Sb/TiO₂.

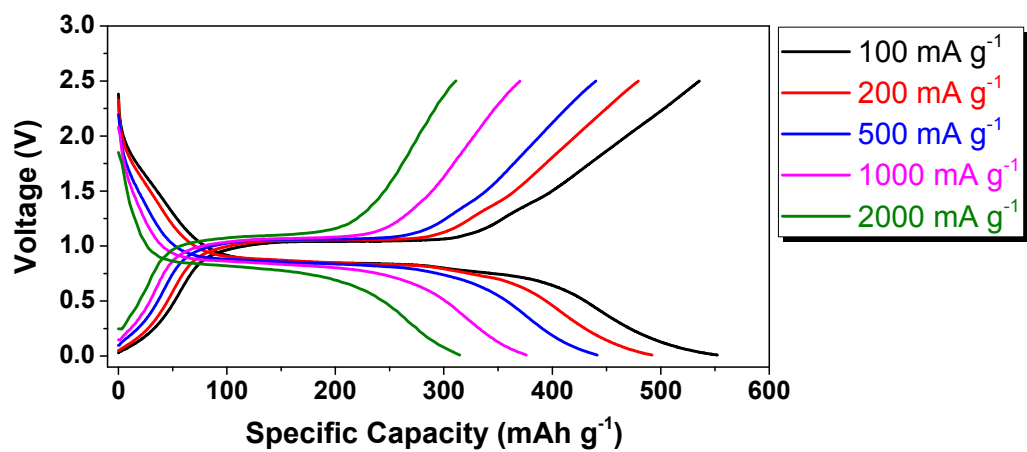


Figure S4 | Typical voltage vs. capacity profiles of hollow interwoven structured Sb/TiO₂ in rate capability test for lithium battery.

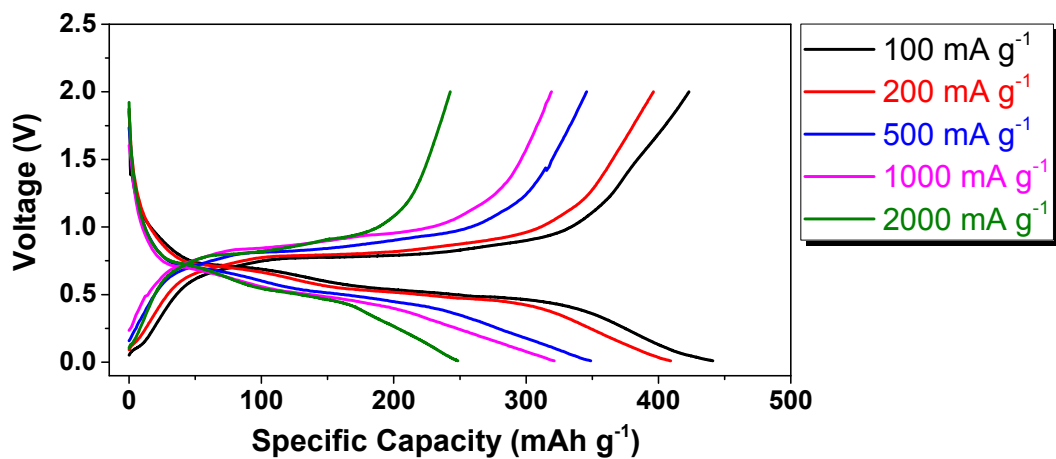


Figure S5 | Typical voltage vs. capacity profiles of hollow interwoven structured Sb/TiO₂ in rate capability test for sodium battery.

Table S2 Comparison of the electrochemical performances of hollow interwoven structured Sb/TiO₂ and those of the previous Sb-based composites as anode in lithium ion battery (LIBs) and sodium ion batteries (SIBs) (where define 1C = 660mA g⁻¹).

Materials	LIBs/SIBs	Current density	Cycle numbers	Capacity (mAh g ⁻¹)	References
Sb@TiO ₂	LIBs	0.15C	100	450	16
Sb/TiO _x /C	LIBs	0.15C	100	408	17
Sb/AlO _x /C	LIBs	0.15C	100	431	17
Sb/MoO _x /C	LIBs	0.15C	100	376	17
Sb/Al ₂ O ₃ /C	LIBs	0.15C	300	440	18
Sb/TiO ₂ /C	LIBs	0.15C	300	445	19
FeSb ₂ /Al ₂ O ₃ /C	LIBs	0.15C	500	350	20
NiSb/Al ₂ O ₃ /C	LIBs	0.15C	100	300	21
Sb/TiO ₂	LIBs	0.15C	100	475	This Work
Sb@C	SIBs	0.15C	500	385	22
I-Sb/rGo	SIBs	0.75C	150	173	23
Sb-C-Go	SIBs	0.15C	100	274	24
Sb/C	SIBs	0.15C	100	372	25
Sb/TiO ₂	SIBs	0.15C	100	403	This work

References

1. Li, Z.; Zhang, J.; Guan, B.; Wang, D.; Liu, L.-M.; Lou, X. W.; A Sulfur Host Based on Titanium Monoxide@Carbon Hollow Spheres for Advanced Lithium-Sulfur Batteries. *Nat. Commun.* **2016**, *7*, 13065-13076.
2. Zhao, S.; Wang, Z.; He, Y.; Jiang, B.; Harn, Y.; Liu, X.; Yu, F.; Feng, F.; Shen, Q.; Lin, Z.; Interconnected Ni(HCO₃)₂ Hollow Spheres Enabled by Self-Sacrificial Templating with Enhanced Lithium Storage Properties. *ACS Energy Lett.* **2017**, *2*, 111-116.
3. Zhang, H.; Noonan, O.; Huang, X.; Yang, Y.; Xu, C.; Zhou, L.; Yu, C.; Surfactant-Free Assembly of Mesoporous Carbon Hollow Spheres with Large Tunable Pore Sizes. *ACS Nano* **2016**, *10*, 4579-4586.
4. Wang, G.; Liang, K.; Liu, L.; Yu, Y.; Hou, S.; Chen, A.; Fabrication of Monodisperse Hollow Mesoporous Carbon Spheres by Using “Confined Nanospace Deposition” Method for Supercapacitor. *J. Alloy. Compd.* **2018**, *736*, 35-41.
5. Liu, H.; Li, W.; Shen, D.; Zhao, D.; Wang, G.; Graphitic Carbon Conformal Coating of Mesoporous TiO₂ Hollow Spheres for High-Performance Lithium Ion Battery Anodes. *J. Am. Chem. Soc.* **2015**, *137*, 13161-13166.
6. Hu, Y.; Jensen, J. O.; Zhang, W.; Cleemann, L. N.; Xing, W.; Bjerrum, N. J.; Li, Q. F.; Hollow Spheres of Iron Carbide Nanoparticles Encased in Graphitic Layers as Oxygen Reduction Catalysts. *Angew. Chem.* **2014**, *53*, 3675-3679.
7. Xia, X. H.; Tu, J. P.; Wang, X. L.; Gu, C. D.; Zhao, X. B.; Mesoporous Co₃O₄ Monolayer Hollow-Sphere Array as Electrochemical Pseudocapacitor Material. *Chem. Commun.* **2011**, *47*, 5786-5788.
8. Liang, K.; He, W.; Deng, X.; Ma, H.; Xu, X.; Controlled Synthesis of NiCo₂S₄ Hollow Spheres as High-Performance Electrode Materials for Supercapacitors. *J. Alloy. Compd.* **2018**, *735*, 1395-1401.
9. Zhang, D.; Sun, W.; Zhang, Y.; Dou, Y.; Jiang, Y.; Dou, S. X.; Engineering Hierarchical Hollow Nickel Sulfide Spheres for High-Performance Sodium Storage. *Adv. Funct. Mater.* **2016**, *26*, 7479-7485.
10. Wang, N.; Zhao, P.; Zhang, Q.; Yao, M.; Hu, W.; Monodisperse Nickel/Cobalt Oxide Composite Hollow Spheres with Mesoporous Shell for Hybrid Supercapacitor: A Facile Fabrication and Excellent Electrochemical Performance. *Compos. Part B-Eng.* **2017**, *113*, 144-151.

11. Zhou, D.; Yang, L.; Yu, L.; Kong, J.; Yao, X.; Liu, W.; Xu, Z.; Lu, X.; Fe/N/C Hollow Nanospheres by Fe(III)-Dopamine Complexation-Assisted One-Pot Doping as Nonprecious-Metal Electrocatalysts for Oxygen Reduction. *Nanoscale* **2015**, *7*, 1501-9.
12. Li, J.; Tang, P.; Zhang, J.; Feng, Y.; Luo, R.; Chen, A.; Li, D.; Facile Synthesis and Acetone Sensing Performance of Hierarchical SnO₂ Hollow Microspheres with Controllable Size and Shell Thickness. *Ind. Eng. Chem. Res.* **2016**, *55*, 3588-3595.
13. Ruckdeschel, P.; Kemnitzer, T. W.; Nutz, F. A.; Senker, J.; Retsch, M.; Hollow Silica Sphere Colloidal Crystals: Insights Into Calcination Dependent Thermal Transport. *Nanoscale* **2015**, *7*, 10059-10070.
14. Tang, C.; Wang, D.; Wu, Z.; Duan, B.; Tungsten Carbide Hollow Microspheres as Electrocatalyst and Platinum Support for Hydrogen Evolution Reaction. *Int. J. Hydrogen Energ.* **2015**, *40*, 3229-3237.
15. Pan, J.; Zhong, L.; Li, M.; Luo, Y.; Li, G.; Microwave-Assisted Solvothermal Synthesis of VO₂ Hollow Spheres and Their Conversion into V₂O₅ Hollow Spheres with Improved Lithium Storage Capability. *Chem. Eur. J.* **2016**, *22*, 1461-1466.
16. Yi, Z.; Han, Q. G.; Ju, S. S.; Wu, Y. M.; Cheng, Y.; Wang, L. M. Fabrication of One-Dimensional Sb@TiO₂ Composites as Anode Materials for Lithium-Ion Batteries. *J. Electrochem. Soc.* **2016**, *163*, A2641-A2646.
17. Yoon, S.; Manthiram, A. Sb-MO_x-C (M = Al, Ti, or Mo) Nanocomposite Anodes for Lithium-Ion Batteries. *Chem. Mater.* **2009**, *21*, 3898-3904.
18. Sung, J. H.; Park, C.-M. Amorphized Sb-based Composite for High-performance Li-ion Battery Anodes. *J. Electroanal. Chem.* **2013**, *700*, 12-16.
19. Hyun Sung, J.; Park, C. M. Sb-based Nanostructured Composite with Embedded TiO₂ for Li-Ion Battery Anodes. *Mater. Lett.* **2013**, *98*, 15-18.
20. Allcorn, E.; Manthiram, A. FeSb₂-Al₂O₃-C Nanocomposite Anodes for Lithium-Ion Batteries. *ACS Appl. Mater. Interfaces* **2014**, *6*, 10886-10891.
21. Allcorn, E.; Manthiram, A. NiSb-Al₂O₃-C Nanocomposite Anodes with Long Cycle Life for Li-Ion Batteries. *J. Phys. Chem. C* **2014**, *118*, 811-822.
22. Zhang, N.; Liu, Y.; Lu, Y.; Han, X.; Cheng, F.; Chen, J. Spherical Nano-Sb@C Composite as a High-rate and Ultra-stable Anode Material for Sodium-ion Batteries. *Nano Res.* **2015**, *8*, 3384-3393.
23. Wan, F.; Lü, H.-Y.; Zhang, X. H.; Liu, D. H.; Zhang, J. P.; He, X.; Wu, X. L. The *In-situ*-prepared micro/nanocomposite Composed of Sb and Reduced Graphene Oxide as Superior Anode for Sodium-ion Batteries. *J. Alloy Compd.* **2016**, *672*, 72-78.

24. Li, K.; Su, D.; Liu, H.; Wang, G. Antimony-Carbon-Graphene Fibrous Composite as Freestanding Anode Materials for Sodium-ion Batteries. *Electrochimica Acta* **2015**, *177*, 304-309.
25. Duan, J.; Zhang, W.; Wu, C.; Fan, Q.; Zhang, W.; Hu, X.; Huang, Y. Self-wrapped Sb/C Nanocomposite as Anode Material for High-Performance Sodium-Ion Batteries. *Nano Energy* **2015**, *16*, 479-487.